Pankaj Thakur[*], *Priya Gulial*

EXPLORING THE INTERPLAY OF STRESS FACTORS IN THIN ROTATING DISK WITH INCLUSIONS AND LOADING EDGES: A COMPREHENSIVE INVESTIGATION

ISTRAŽIVANJE ULOGE FAKTORA NAPONA KOD TANKOG ROTIRAJUĆEG DISKA SA UKLJUČCIMA I IVIČNIM OPTEREĆENJEM: SVEOBUHVATNO ISTRAŽIVANJE

Originalni naučni rad / Original scientific paper
Rad primljen / Paper received: 16.02.2024
https://doi.org/10.69644/ivk-2025-02-0285

Adresa autora / Author's address:
Department of Mathematics, ICFAI University, Himachal Pradesh, India *email: pankaj_thakur15@yahoo.co.in
P. Thakur https://orcid.org/0000-0001-8119-2697 ;
P. Gulial https://orcid.org/0009-0009-0266-2298

Keywords
- stress
- density
- disk
- isotropic
- shaft

Ključne reči
- napon
- gustina
- disk
- izotropan
- osovina

Abstract

This study investigates the complex interplay of stress factors in thin rotating disks with inclusions and loading edges. Thin disks are ubiquitous in various engineering applications, and understanding their behaviour under rotational forces is crucial for design optimisation and structural integrity. In this research we systematically vary parameters such as inclusion size, material properties, and loading conditions to comprehensively analyse their effects on stress distribution within the disk. Through advanced mathematical modelling, we provide insights into the interaction between inclusions, loading edges, and rotational forces, shedding light on critical factors influencing disk performance and durability. This comprehensive investigation contributes to the advancement of design methodologies for thin rotating structures in engineering applications.

Izvod

U ovom radu istražujemo složenu ulogu faktora napona kod tankog rotirajućeg diska sa uključcima i sa ivičnim opterećenjem. Tanki diskovi su sveprisutni u raznim inženjerskim primenama, a razumevanje njihovog ponašanja u uslovima sila rotacije je od značaja za optimizaciju projektovanja i integriteta konstrukcije. U ovom istraživanju sistematski variramo parametre kao što su veličina uključka, osobine materijala i uslove opterećenja, kako bismo sveobuhvatno analizirali njihove uticaje na raspodelu napona u disku. Naprednijim matematičkim modeliranjem dobijamo uvid u interakcije između uključaka, ivičnog opterećenja i sila rotacije, i time rasvetljavamo uticaje kritičnih faktora na performanse i izdržljivost diska. Ovo sveobuhvatno istraživanje doprinosi razvoju metodologije projektovanja tankih rotirajućih konstrukcija u inženjerskim primenama.

INTRODUCTION

Rotating disks are ubiquitous in various engineering applications, ranging from aerospace propulsion systems to industrial machinery. Understanding the stress distribution in these disks is paramount for ensuring their structural integrity and optimal performance. This introduction delves into the intricate interplay of stress factors in thin rotating disks, particularly focusing on the influence of inclusions and loading edges. By embarking on a comprehensive investigation, this study aims to unravel the complex mechanisms governing stress distribution in such disks, shedding light on crucial insights for engineering design and analysis. Thin rotating disks, characterised by their relatively small thickness compared to their diameter, are prone to experiencing significant stress concentrations under rotational forces. These stresses can arise from various factors, including centrifugal forces, thermal gradients, and mechanical loading. In addition to these inherent stress sources, the presence of inclusions within the disk material and loading edges further complicates the stress distribution pattern. Inclusions, or internal defects within the material, are common in manufacturing processes and can significantly influence the mechanical properties of the disk. Depending on their size, shape, and distribution, inclusions can act as stress concentrators, exacerbating the localized stress levels and potentially leading to premature failure. Understanding the interaction between these inclusions and the surrounding material under rotational conditions is crucial for predicting the disk's structural response. Furthermore, loading edges play a pivotal role in determining the stress distribution in rotating disks. These edges, where external loads are applied, introduce additional complexities into the stress analysis. The manner in which the applied loads are distributed along the edges, coupled with the rotational motion of the disk, results in non-uniform stress profiles across its surface. Consequently, accurately characterising the stress distribution near the loading edges is essential for assessing the disk's structural integrity and ensuring safe operating conditions. The comprehensive investigation proposed in this study aims to address the aforementioned challenges by employing advanced analytical and numerical techniques. Finite element analysis (FEA) and computational fluid dynamics (CFD) simulations will be utilised to model the intricate behaviour of thin rotating disks with inclusions and loading edges. These numerical simulations will be complemented by theoretical analyses based on principles of solid mechanics and fluid dynamics, providing a multi-faceted understanding of the stress factors at play. Moreover, experimental validation will be conducted to corroborate the findings from numerical and theoretical analyses. Experimental techniques such as strain gauging, optical interferometry, and acoustic emission testing will be employed to measure the actual stress distribution and deformation patterns in rotating disks subjected to controlled loading conditions. By integrating experimental data with numerical simulations, this study aims to enhance the accuracy and reliability of the stress analysis methodology. The analysis of thin rotating disks crafted from isotropic material has been thoroughly examined by Timoshenko and Goodier /1/ in the elastic realm, and by Chakrabarty /2/ and Heyman /3/ for the plastic domain. Güven /4/, meanwhile, delved into the issue of rigid inclusion under the premises of Tresca's yield condition, its corresponding flow rule, and linear strain hardening. In securing the stress distribution, Güven aligned the plastic stresses at identical radii of the disk. Seth 5/ has defined the generalised principal strain measure as:

$$e_{ii} = \int_0^{\overset{A}{e}_{ii}} \left[1-2\overset{A}{e}_{ii}\right]^{\frac{n}{2}-1} d\overset{A}{e}_{ij} = \frac{1}{n}\left[1-\left(1-2\overset{A}{e}_{ii}\right)^{\frac{n}{2}}\right],\quad i = 1, 2, 3. \quad (1)$$

In this context, n represents the measure, while $\overset{A}{e}_{ii}$ denotes the principal Almansi finite strain components, with values $n = -2, -1, 0, 1, 2$ corresponding to Cauchy, Green-Hencky, Swainger, and Almansi measures, respectively.

OBJECTIVE OF THE STUDY

The objective of this study is to conduct a thorough investigation into the intricate interplay of stress factors in thin rotating disks characterised by the presence of both inclusions and loading edges. Thin rotating disks are commonly utilised in various engineering applications such as turbines, rotors, and flywheels, where they are subjected to complex loading conditions. The presence of inclusions which are typically rigid structures embedded within the disk material, introduces additional stress concentrations and alters the overall stress distribution within the disk. Furthermore, the loading edges of the disk play a crucial role in determining its structural integrity and performance under rotational forces. By comprehensively examining the interaction between stress factors in such disks, this study aims to provide valuable insights into their mechanical behaviour and failure mechanisms. This includes analysing the effects of different parameters such as disk geometry, material properties, inclusion size and shape, and loading conditions on the stress distribution and overall structural response. The findings of this investigation will not only contribute to a better understanding of the mechanical behaviour of thin rotating disks with inclusions and loading edges but also have practical implications for the design and optimisation of such components in engineering applications. Through advanced analytical and numerical techniques, this study seeks to address the complexities associated with these systems and provide meaningful recommendations for their improved performance and reliability.

PROBLEM FORMULATION

A thin disk of constant density, featuring a central bore with inner radius a, and outer radius b, is under consideration. This annular disk is affixed to a rigid shaft, experiencing edge loading. The disk rotates at angular speed ω about an axis perpendicular to its plane, traversing through the centre. The disk thickness is assumed to remain constant and is considered sufficiently small to maintain a state of plane stress, where the axial stress T_{zz} is negligible.

Boundary conditions: the disk under investigation in this study has a constant density and is subjected to a load. The inner surface of the disk is presumed to be fixed to a shaft, while the outer surface of the disk experiences a mechanical load. Consequently, the boundary conditions of the problem are defined as follows:

$$u = 0 \text{ at } r = a \text{ and } T_{rr} = T_0 \text{ at } r = b, \quad (2)$$

and $p_{int.}$ is pressure applied at the disk inner surface.

BASIC GOVERNING EQUATION

The problem formulation entails expressing the displacement components in cylindrical polar coordinates as follows /6, 7/:

$$u = r(1-\beta),\ v = 0,\ w = dz\,. \quad (3)$$

Stress components are given /6-8/ by using Eq.(1), we get:

$$T_{rr} = \frac{2\mu}{n}[3-2C-\beta^n\{1-C+(2-C)(P+1)^n\}],$$

$$T_{\theta\theta} = \frac{2\mu}{n}[3-2C-\beta^n\{2-C+(1-C)(P+1)^n\}],$$

$$T_{r\theta} = T_{\theta z} = T_{zr} = T_{zz} = 0\,, \quad (4)$$

where: $r\beta' = \beta\eta$ (η is function of β, and β is function of r); and $c = 2\mu/(\lambda + 2\mu)$. For an isotropic disk centrifugal forces are zero, therefore equations of equilibrium become:

$$\frac{d}{dr}(rT_{rr}) - T_{\theta\theta} + \rho\omega^2 r^2 = 0\,. \quad (5)$$

By employing Eq.(4) into Eq.(5), we obtain a nonlinear differential equation in β as follows:

$$n(2-c)\beta^{n+1}P(P+1)^{n-1}\frac{dP}{d\beta} = \frac{n\rho\omega^2 r^2}{2\mu} + \beta^n \times$$
$$\times[1-(1+P)^n - np\{1-c+(2-c)(1+P)^n\}]\,, \quad (6)$$

where: $\beta' = d\beta/dr$.

ELASTIC TO PLASTIC SOLUTIONS

To determine the plastic stress, the transition function is aligned with the principal stress at the transition point, as outlined in Seth /6, 7/, and Thakur /8-25/. The transition function R is defined as follows:

$$R = T_{\theta\theta} = \left(\frac{2\mu}{n}\right)[(3-2C)-\beta^n\{2-C+(1-C)(P+1)^n\}]\,. \quad (7)$$

When we perform logarithmic differentiation of Eq.(7) with respect to r and utilize Eq.(6), after that taking $\beta \to \pm\infty$ and then integrating, we get the result is:

$$R = A_1 r^{-1/(2-C)}\,. \quad (8)$$

Therefore, Eqs. (7) and (8) become:

$$T_{\theta\theta} = \left(\frac{2\mu}{n}\right)A_1 r^{-1/(2-C)}\,. \quad (9)$$

Upon substituting Eq.(9) into Eq.(5) and performing the integration, we obtain

$$T_{rr} = \left\{\frac{2\mu(2-C)}{n(1-C)}\right\}A_1 r^{-1/(2-C)} - \frac{\rho\omega^2 r^2}{3} + \frac{B_1}{r}\,. \quad (10)$$

By substituting Eqs. (9) and (10) into

$$e_{\theta\theta}=\frac{u}{r}-\frac{u^2}{2r^2}=\frac{1}{2}[1-\beta^2]=\frac{1}{E}\left[T_{\theta\theta}-\left(\frac{1-C}{2-C}\right)T_{rr}\right],$$

we obtain $$\beta=\sqrt{1-\frac{2(1-C)}{E(2-C)}\left[\frac{\rho\omega^2r^2}{3}-\frac{B_1}{r}\right]}. \qquad (11)$$

Inserting Eq.(11) into Eq.(3), we get

$$u=r-r\sqrt{1-\frac{2(1-C)}{E(2-C)}\left[\frac{\rho\omega^2r^2}{3}-\frac{B_1}{r}\right]}. \qquad (12)$$

By applying boundary condition Eq.(2) into Eqs.(10) and (12), we obtain

$$A_1=\frac{n\nu}{2\mu b^\nu}\left[bT_0+\frac{\rho\omega^2(b^3-a^3)}{3}\right],\ B_1=\frac{\rho\omega^2a^3}{3}. \qquad (13)$$

Upon substituting Eq.(13) into Eqs. (9), (10), and (12), in respect, we derive the transitional stresses and displacement as follows:

$$T_{\theta\theta}=\frac{\nu}{r}\left(\frac{r}{b}\right)^\nu\left[bT_0+\frac{\rho\omega^2(b^3-a^3)}{3}\right],$$

$$T_{rr}=\left(\frac{r}{b}\right)^{\nu-1}T_0+\frac{\rho\omega^2}{3r}\left[\left(\frac{r}{b}\right)^\nu(b^3-a^3)-r^3+a^3\right],$$

$$u=r-r\sqrt{1-\frac{2\nu}{E}\frac{\rho\omega^2(r^3-a^3)}{3r}},$$

$$T_{rr}-T_{\theta\theta}=\left(\frac{r}{b}\right)^{\nu-1}(1-\nu)T_0+\frac{\rho\omega^2}{3r}\times$$
$$\times\left\{\left(\frac{r}{b}\right)^\nu(b^3-a^3)(1-\nu)-r^3+a^3\right\}. \qquad (14)$$

Initial yielding: Eq.(14) reveals that $|T_{rr}-T_{\theta\theta}|$ reaches its maximum value at the internal surface (i.e., r = a). Consequently, yielding occurs at the internal surface of the disk, and Eq.(14) yields:

$$\left|T_{rr}-T_{\theta\theta}\right|_{r=a}=\left|\left(\frac{a}{b}\right)^{\nu-1}(1-\nu)T_0+\frac{\rho\omega^2}{3a}\left(\frac{a}{b}\right)^\nu(b^3-a^3)(1-\nu)\right|\equiv Y(\text{say})$$

The angular speed required for initial yielding is determined by:

$$\Omega_i^2=\frac{\rho\omega_i^2b^2}{Y}=\left|\frac{3ab^2\left[1-\sigma_0(1-\nu)\left(\frac{a}{b}\right)^{\nu-1}\right]}{\left(\frac{a}{b}\right)^\nu(b^3-a^3)(1-\nu)}\right|. \qquad (15)$$

State of complete plasticity: the rotational velocity at which the rotating disk reaches full plasticity at its outer surface, leads to a transformation in Eq.(14):

$$\left|T_{rr}-T_{\theta\theta}\right|_{r=b}=\left|\frac{T_0}{2}-\frac{\rho\omega^2}{6b}(b^3-a^3)\right|\equiv Y^*(\text{say}),$$

where: Y^* represents the yielding stresses present in a fully-plastic state, and the angular velocity needed for the disk to attain full plasticity is described by:

$$\Omega_f^2=\frac{\rho\omega_f^2b^2}{Y^*}=\left|6\frac{(\sigma_0/2)-1)}{1-(a^3/b^3)}\right|. \qquad (16)$$

We introduce the ensuing dimensionless constituents: $R=r/b$, $R_0=a/b$, $\sigma_r=T_{rr}/Y$, $\sigma_\theta=T_{\theta\theta}/Y$, $U=u/b$, $\Omega^2=\rho_0\omega^2b^2/Y$, $\sigma_0=T_0/Y$, and $H=Y/E$. Elastic-plastic transitional stresses, displacement, and angular velocity derived from Eqs. (14) and (15) transform into their non-dimensional representations:

$$\sigma_\theta=\nu R^{\nu-1}\left[\sigma_0+\frac{\Omega_i^2}{3}(1-R_0^3)\right],$$

$$\sigma_r=\sigma_0R^{\nu-1}+\frac{\Omega_i^2}{3R}\left[R^\nu(1-R_0^3)-R^3+R_0^3\right], \qquad (17)$$

$$U=R-R\sqrt{1-\frac{2\nu H\Omega_i^2}{3R}(R^3-R_0^3)},$$

and $$\Omega_i^2=\frac{3[1-\sigma_0(1-\nu)R_0^{\nu-1}]}{R_0^{\nu-1}(1-R_0^3)(1-\nu)}. \qquad (18)$$

The stresses, displacement, and angular speed for a fully-plastic state are derived from Eqs. (17) and (18) as follows:

$$\sigma_\theta=\frac{1}{2\sqrt{R}}\left[\sigma_0+\frac{\Omega_f^2}{3}(1-R_0^3)\right],$$

$$\sigma_r=\frac{\sigma_0}{\sqrt{R}}+\frac{\Omega_f^2}{3R}[\sqrt{R}(1-R_0^3)-R^3+R_0^3],$$

$$U_f=R-R\sqrt{1-\frac{H\Omega_i^2}{3R}(R^3-R_0^3)},$$

$$\Omega_f^2=\frac{\rho\omega_f^2b^2}{Y^*}=\frac{6\left(1-\frac{\sigma_0}{2}\right)}{1-R_0^3}. \qquad (19)$$

VALIDATION OF RESULTS

Equations (17)-(19) correspond identically to those presented by Thakur /8/ under the condition where no load is applied to the rotating disk containing rigid inclusions.

RESULTS AND DISCUSSION

To determine the stresses, angular speed, and displacement using the aforementioned analysis, the following values are selected: C = 0.00, 0.25, 0.5; E/Y = 0.125; and σ_0 = 0, 0.115, and 0.25, correspondingly. Furthermore, Table 1 illustrates that in order for an incompressible material to attain full plasticity, a higher percentage increase in angular velocity is necessary compared to a rotating disk comprised of compressible material. Figure 1 illustrates curves plotting the angular speed needed for initial yielding against various ratios of radii, considering C values of 0, 0.25, and 0.5, as well as α values of 0, 0.125, and 0.2, for a disk containing rigid inclusions. It is noted that in the absence of loading, rotating disks with inclusions require significantly higher angular speeds for incompressible materials compared to compressible materials. With the introduction of edge loading, lower angular speed values are required to induce yielding at the internal surface for both incompressible and compressible materials. In Figs. 2 and 3, curves are depicted for stress distribution and displacement relative to radius ratio $R=r/b$ for the elastic-plastic transitional state and fully plastic state, in respect. It is observed that radial stresses reach their maximum value at the internal surface of rotating disks made of incompressible material compared to compressible material. Furthermore, with the effect of edge loading, radial stresses are expected to decrease with increasing values of edge load in both the elastic-plastic and fully plastic states.

Table 1. Angular velocity needed for initial yielding and complete plasticity under various load conditions.

Load σ_0	Material compressibility	Initial yielding necessitates a specific angular velocity Ω_i^2	Angular velocity needed for a fully plastic state Ω_f^2	Percentage rise in angular velocity $\left(\sqrt{\frac{\Omega_f^2}{\Omega_i^2}}-1\right)\times 100$
0	0	4.8	6.8	19 %
0.125	0	4.4	6.4	20.6 %
0.2	0	4.2	6.2	21.8 %
0	0.25	4.04	6.9	30.3 %
0.125	0.25	3.6	6.4	33.5 %
0.2	0.25	3.4	6.2	35.7 %
0	0.5	3.2	6.9	45.5 %
0.125	0.5	2.8	6.4	51.2 %
0.2	0.5	2.6	6.2	55.5 %

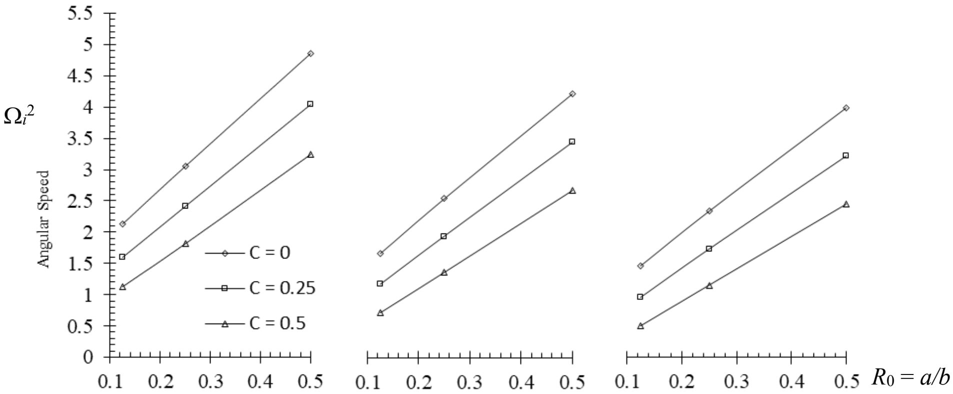

Figure 1. Angular speed vs. radii ratio R_0.

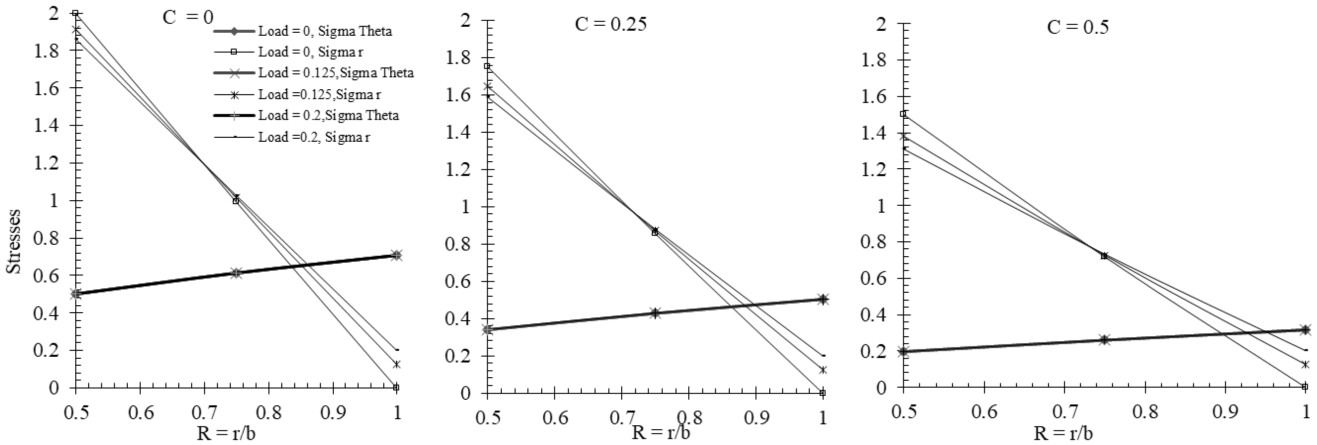

Figure 2. Stresses for initial yielding vs. radii ratio $R = r/b$.

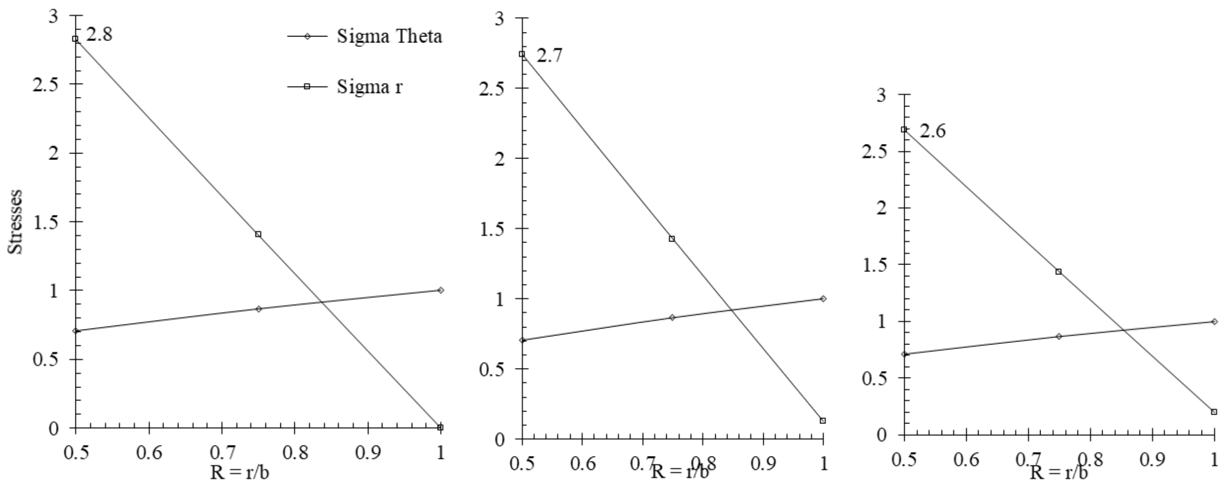

Figure 3. Stresses for fully-plastic state vs. radii ratio $R = r/b$.

CONCLUSIONS

The main findings are as follows.

- In the absence of load, rotating disks with inclusions require significantly higher angular speeds for incompressible materials compared to compressible materials.
- Introduction of edge loading reduces the required angular speed to induce yielding at the internal surface for both incompressible and compressible materials.
- Radial stresses reach their maximum value at the internal surface of rotating disks made of incompressible material compared to compressible material.
- With the effect of edge loading, radial stresses decrease with increasing values of edge load in both the elastic-plastic and fully plastic states.

ACKNOWLEDGEMENT

This research article is especially dedicated to Prof. Dr. Aleksandar Sedmak (editor-in-chief Emeritus) and Prof. Zoran Radaković (editor-in-chief) of *Structural Integrity and Life* journal and the Society for Structural Integrity and Life 'Prof. Dr. Stojan Sedmak', IMS Institute, Serbia.

REFERENCES

1. Timoshenko, S.P., Goodier, J.N., Theory of Elasticity, 3rd Ed., McGraw-Hill Book Co., New York, USA, 1970.
2. Chakrabarty, J., Theory of Plasticity, McGraw-Hill, New York, 1987.
3. Heyman J., (1958), *Plastic design of rotating discs*, Proc. Inst. Mech. Eng. 172(1): 531-547. doi: 10.1243/PIME_PROC_1958_172_045
4. Güven, U. (1998), *Elastic-plastic stress distribution in a rotating hyperbolic disk with rigid inclusion*, Int. J Mech. Sci. 40(1): 97-109. doi: 10.1016/S0020-7403(97)00036-2
5. Güven, U. (1999), *Elastic-plastic rotating disk with rigid inclusion*, Mech. Struct. Machines, 27(1): 117-128. doi: 10.1080/08905459908915691
6. Seth, B.R. (1962), *Transition theory of elastic-plastic deformation, creep and relaxation*, Nature, 195: 896-897. doi:10.1038/195896a0
7. Seth, B.R. (1966), *Measure concept in mechanics*, Int. J Nonlinear Mech., 1(1): 35-40. doi: 10.1016/0020-7462(66)90016-3
8. Thakur, P., *Some problems in elastic-plastic and creep transition*, Ph.D. Thesis, Dept. of Mathematics and Statistics, Himachal Pradesh University, Shimla, India, 2006 https://shodhganga.inflibnet.ac.in/handle/10603/121294
9. Thakur, P., Sethi, M., Kumar, N., et al. (2021), *Analytical solution of hyperbolic deformable disk having variable density*, Mech. Solids, 56(6): 1039-1046. doi: 10.3103/S0025654421060194
10. Sethi, M., Thakur, P. (2020), *Elastoplastic deformation in an isotropic material disk with shaft subjected to load and variable density*, J Rubber Res. 23: 69-78. doi: 10.1007/s42464-020-00038-8
11. Thakur, P., Gupta N., Sethi, M., Gupta K. (2020), *Effect of density parameter in a disk made of orthotropic material and rubber*, J Rub. Res. 23(3): 193-201. doi: 10.1007/s42464-02 0-00049-5
12. Thakur, P., Kumar, N., Sukhvinder (2020), *Elasto-plastic density variation in a deformable disk*, Struct. Integr. Life, 20 (1): 27-32.
13. Thakur, P., Sethi M. (2020), *Elastoplastic deformation in an orthotropic spherical shell subjected to temperature gradient*, Math. Mech. Solids, 25(1): 26-34. doi: 10.1177/1081286519857128
14. Thakur, P., Sethi, M., Gupta, K., Bhardwaj, R.K. (2021), *Thermal stress analysis in a hemispherical shell made of transversely isotropic materials under pressure and thermo-mechanical loads*, J Appl. Math. Mech. (ZAMM), 101(12). doi: 10.1002/zamm.202100208
15. Thakur, P., Kumar, N., Sethi, M. (2021), *Elastic-plastic stresses in a rotating disc of transversely isotropic material fitted with a shaft and subjected to thermal gradient*, Meccanica, 56: 1165-1175. doi: 10.1007/s11012-021-01318-2
16. Thakur, P., Sethi, M., Gupta, N., Gupta, K. (2021), *Thermal effects in rectangular plate made of rubber, copper and glass materials*, J Rubber Res. 24(1): 147-155. doi: 10.1007/s42464-020-00080-6
17. Thakur, P., Sethi, M., Kumar, N., et al. (2021), *Thermal effects in a rotating disk made of rubber and magnesium materials and having variable density*, J Rubber Res. 24(3): 403-413. doi: 10.1007/s42464-021-00107-6
18. Thakur, P., Sethi, M., Kumar, N., et al. (2021), *Analytical solution of hyperbolic deformable disk having variable density*, Mech. Solids, 56(6): 1039-1046. doi: 10.3103/S0025654421060194
19. Kumar, N., Thakur, P. (2021), *Thermal behaviour in a rotating disc made of transversely isotropic material with rigid shaft*, Struct. Integr. Life, 21(3): 217-223.
20. Thakur, P., Kumar, N., Gupta, K. (2022), *Thermal stress distribution in a hyperbolic disk made of rubber/brass material*, J Rubber Res. 25(1): 27-37. doi: 10.1007/s42464-022-00147-6
21. Thakur, P., Sethi, M., Kumar, N., et al. (2022), *Stress analysis in an isotropic hyperbolic rotating disk fitted with rigid shaft*, Z Angew. Math. Phys. 73(1), Art. ID 23. doi: 10.1007/s00033-021-01663-y
22. Kumar, A., Sood, S., Thakur, P., Kumar, N. (2022), *Safety analysis in an isotropic material disc fitted with a rigid shaft subjected to thermo-mechanical load by using transition theory*, Struct. Integr. Life, 22(2): 193-201.
23. Kumar, N., Thakur, P. (2022), *Behaviour of creep stress and strain rates in a solid disc made of isotropic material with thermal condition*, Struct. Integr. Life, 22(2): 202-209.
24. Chand, S., Sood, S., Thakur, P., Gupta, K. (2023), *Elastoplastic stress deformation in an annular disk made of isotropic material and subjected to uniform pressure*, Struct. Integr. Life, 23 (1): 61-64.
25. Singh, N., Kaur, J., Thakur, P., Murali, G. (2023), *Structural behaviour of annular isotropic disk made of steel/copper material with gradually varying thickness subjected to internal pressure*, Struct. Integr. Life, 23(3): 293-297.